Available online at www.sciencedirect.com
ScienceDirect
Journal of the European Ceramic Society 26 (2006) 3273–3278
www.elsevier.com/locate/jeurceramsoc

Structural, chemical and dielectric properties of ceramic injection moulded $Ba(Zn_{1/3}Ta_{2/3})O_3$ microwave dielectric ceramics

Shaojun Liu [a], Vincent A. Merrick [b], N. Newman [a,*]

[a] *Chemical and Materials Engineering Department, Arizona State University, Tempe, AZ 85287, USA*
[b] *Valley Pattern & Mold Co., Inc., Tempe, AZ 85283-3652, USA*

Received 23 February 2005; received in revised form 25 July 2005; accepted 4 August 2005
Available online 29 September 2005

Abstract

We report the development of a ceramic injection moulding (CIM) process to produce complex-shaped structures using high-performance microwave ceramic materials. In particular, we describe the synthesis methods and the structural, chemical and dielectric properties of $Ba(Zn_{1/3}Ta_{2/3})O_3$ (BZT) doped with Ni and Zr ceramics produced using ceramic injection moulding. Sintering the ceramic injection moulded $Ba(Zn_{1/3}Ta_{2/3})O_3$ to a relative density of ~94% was possible at a temperature of 1680 °C and a time of 48 h. The best samples to date exhibit a dielectric constant, ε_r, of ~30, a Q value, of ~31,250 (i.e. $\tan\delta < 3.2 \times 10^{-5}$) at 2 GHz, and a temperature coefficient of resonance frequency, τ_f, of 0.1 ppm/°C.

Keywords: Injection moulding; Dielectrics properties; Tantalates; Resonators; $Ba(Zn, Ta)O_3$

1. Introduction

Rapid progress in electromagnetic simulation methods has enabled a significant improvement in the performance of state-of-the-art microwave devices. A growing number of these devices require intricately shaped microwave materials. This has placed increasing demand on the ceramic research community to develop a low-cost process that can manufacture high performance microwave materials in complex-shapes. The use of dielectric ceramics with low loss, high dielectric constants, and near-zero temperature coefficient of resonant frequency is also essential in achieving the required microwave performance for the devices of interest.[1,2] Ni-doped $Ba(Zn_{1/3}Ta_{2/3})O_3$, for example, is commonly used for many microwave materials as it exhibits excellent high frequency properties with a high dielectric constant ($\varepsilon_r \sim 30$), a low loss tangent ($<2 \times 10^{-5}$ at 2 GHz) and has a near-zero temperature coefficient of resonant frequency, τ_f.[3] Zr is often alloyed with this compound since it has been found to improve the manufacturability of the material by allowing shorter annealing times to achieve low loss.[4]

Several traditional ceramics have been successfully manufactured in high volume and with great dimensional precision using ceramic injection molding (CIM), including silicon nitride,[5] zirconia,[6,7] and alumina.[8,9] Another advantage of ceramic injection moulding is that it can economically produce ceramics of complex shapes. However, most research to-date has focused on investigating the mechanical properties of ceramics parts, while little attention has been paid to the electronic and dielectric properties. Further, in this area, no work has so far been published that would concern this technically important microwave dielectric ceramics. For microwave devices for practical applications, it is important that ceramic injection moulded ceramics have sufficiently high dielectric constant, low loss tangent and near zero temperature coefficient of resonant frequency.

Our initial attempts to produce parts with the complex-shaped structure using conventional ceramic forming technology failed as a result of the intrinsic hardness and brittleness of $Ba(Zn_{1/3}Ta_{2/3})O_3$. Through a collaborative effort with Jeff Pond at NRL, we developed methods to fabricate these devices using ceramic injection moulding. In this paper, we report: (a) the development of a ceramic injection moulding process that can produce complicated geometric structures from high-performance microwave dielectrics [i.e. $Ba(Zn_{1/3}Ta_{2/3})O_3$] and (b) the microwave, structural and sintering properties of the materials produced. We have chosen to demonstrate the ceramic

* Corresponding author.
E-mail address: nathan.newman@asu.edu (N. Newman).

0955-2219/$ – see front matter © 2005 Elsevier Ltd. All rights reserved.
doi:10.1016/j.jeurceramsoc.2005.08.001

injection moulding capability by synthesizing a recently proposed microwave high power filter that uses a dual-mode möbius geometry resonator to achieve a four-fold reduction in volume over conventional designs.[10] Further reduction in size is achieved in our device by using dielectric loading with materials exhibiting a high dielectric constant [e.g. ~30 for $Ba(Zn_{1/3}Ta_{2/3})O_3$].[11]

2. Experimental procedure

$Ba(Zn_{1/3}Ta_{2/3})O_3$ doped with Ni and Zr was made from reagent grade $BaCO_3$, ZnO, Ta_2O_5, NiO, and ZrO_2 powders. The raw materials were blended by using ZrO_2 ball milling media and distilled water for 16 h to deagglomerate the powder and provide a homogeneous distribution of raw powder. The slurry was dried and then filtered through 14-mesh screen. It is subsequently heated to 1350 °C for 10 h with an initial ramp of 100 °C/h in air to form single-phase $Ba(Zn_{1/3}Ta_{2/3})O_3$ powder by solid state reaction. For the ceramic injection moulding process, low viscosity feedstock comprised of wax-based binder, ceramic powder and lubricant is used. The binder is composed of paraffin wax, carnauba wax, polyethylene, and stearic acid in a weight ratio of 70:10:19:1. Stearic acid serves as the lubricant in this process. The $Ba(Zn_{1/3}Ta_{2/3})O_3$ powder was loaded to 50 vol.% and the ceramic feedstock was stirred at 130 °C for 4 h to homogenize the mixture of powder and binder. The feedstock was subsequently fed into a plastic injection-moulding machine (Gluco, type LP20, Jenison, MI, USA) to form the Möbius structure with 100 MP pressure at 180 °C. The moulded samples were thermally debound in air with a ramp rate of 20 °C/h up to 700 °C. Note that the organic binder is removed at moderate-temperatures (150–250 °C), and it is important that the ramp rate is sufficiently slow to ensure that this process is complete before exposing the sample to temperatures at which the polymers decompose. The debound samples were then sintered at 1520 °C, 1550 °C, 1580 °C, 1650 °C, or 1680 °C using a ramp rate of 300 °C/h. In order to minimize ZnO evaporation when sintering $Ba(Zn_{1/3}Ta_{2/3})O_3$ at very high temperature, the ceramic injection moulded samples were packed by powder of the same composition and the Pt crucible was sealed with Pt foil.

The structural properties of the samples were characterized using a Rigaku D/MAX-IIB diffractometer equipped with single crystal graphite Cu Kα monochromator. The microstructure of the samples was characterized using a Hitachi S-4200 scanning electron microscope. SEM specimens were prepared for examination in a two-step process in which they were first polished and then a thin gold film was sputter-deposited. The sintered density of high quality samples was measured using the Archimedes method. The bulk density of low-density samples was evaluated by measuring the dimension and weight of the specimen.

The microwave quality factor (Q) and temperature coefficient of resonant frequency (τ_f) were measured using the $TE_{01\delta}$ mode of the dielectric resonator. The $TE_{01\delta}$ mode was measured using S11 reflection data at the terminals of the one port cavity that is connected to a vector network analyzer. The resonator was enclosed in an Au-coated test cavity with dimensions about three times larger than the sample size. Low-loss supports were used to suspend the specimen in the center of the cavity. The quality factor was measured in reflection at room temperature. Microwave coupling was tuned to ~40 dB loss by carefully adjusting the position of the electric probes. The temperature coefficient of resonant frequency τ_f at microwave frequencies was measured between 25 °C and 60 °C.

3. Results and discussion

3.1. X-ray analyses and microstructure

Fig. 1(a) and (b) compares the X-ray diffraction (XRD) patterns of $Ba(Zn_{1/3}Ta_{2/3})O_3$ samples prepared with conventional powder processing and ceramic injection moulding methods. There is not significant structural difference between the two methods for ceramics sintered at 1520 °C and 1680 °C. These two samples do not exhibit ordering, as indicated by absence of additional superstructure peaks in the XRD patterns. Also, there is not evidence of any second phases that would be produced from decomposition as a result of preferential ZnO evaporative loss during sintering. This is important as significant levels of secondary phases can lead to enhanced microwave loss.

Fig. 2 shows the dependence of density on the temperature. The rate of heating during sintering for all the samples was the same (5 °C/min). The low sintering density that was observed after sintering at 1520 °C for 48 h (72%) demonstrated that ceramics injection moulded $Ba(Zn_{1/3}Ta_{2/3})O_3$ does not undergo significant densification under the same conditions that conventional powder processed $Ba(Zn_{1/3}Ta_{2/3})O_3$ samples do (i.e. ~96%). Surprisingly, a sintered density of only ~82% was found after the ceramic injection moulded samples were sintered at 1650 °C. Only when the sample was sintered at 1680 °C does the density achieve a respectable value of ~94%. Thus, high temperatures and extended sintering times had to be used to achieve high density with our $Ba(Zn_{1/3}Ta_{2/3})O_3$ ceramic injection moulding process.

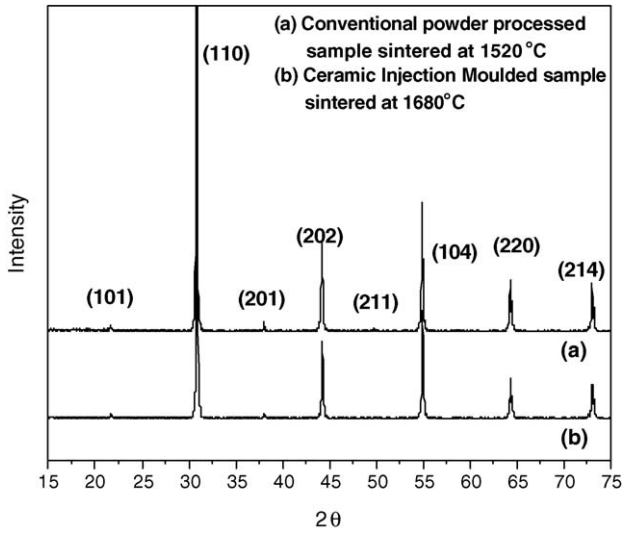

Fig. 1. X-ray diffraction patterns of $Ba(Zn_{1/3}Ta_{2/3})$ doped with Zr and Ni: (a) conventional powder processed sample sintered at 1520 °C and (b) ceramic injection moulded sample sintered at 1680 °C.

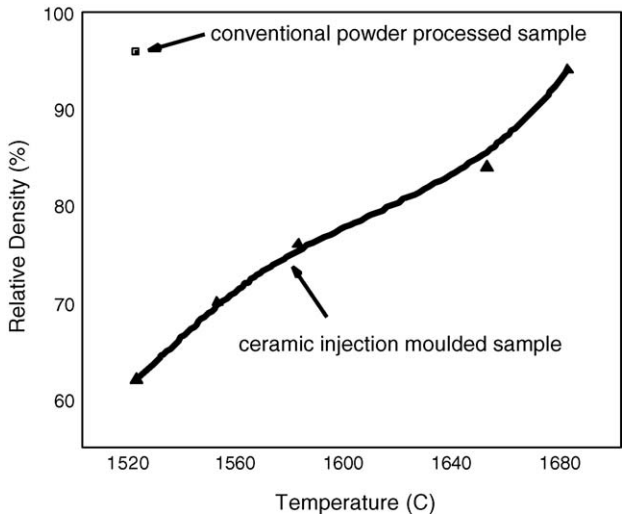

Fig. 2. Dependence of relative density on the sintering temperature for ceramic injection moulded Zr- and Ni-doped $Ba(Zn_{1/3}Ta_{2/3})O_3$. The theoretical density is 7.94 g/cm^3.

Densification usually accompanies the elimination of porosity and grain growth during high temperature sintering. The structure and homogeneity of pores in the powder compact strongly affects the sintering behavior.[12] Agglomerates, in particular, limit the attainable green density, interfere with the development of microstructure, and impede initial-stage sintering kinetics. This is especially characteristic of powder injection moulded samples, which may have poorly dispersed powders in the powder and binder-mixing step.[13,14] Previous investigations have clearly shown that large pores and pore clusters in the sample, as a result of viscous binder flow at the debinding temperature; result in microstructure inhomogeneity, e.g the presence of agglomerate that subsequently affects the diffusion on sintering, in the powder compact, which is often preserved in the final microstructure even after completion of the sintering process.[13,14] Such microstructure inhomogeneity can cause a significant reduction in the driving force for densification.[12,15] We suggest that this is the mechanism responsible for requiring a significantly higher sintering temperature in ceramic injection moulding of $Ba(Zn_{1/3}Ta_{2/3})O_3$ than in conventional ceramic powder processing. Fig. 3(a) is an SEM micrograph of a ceramic injection moulded sample sintered at 1520 °C that shows that there exist a large number of pores with sizes ranging from 2 μm to 4 μm. There is no evidence for densification outside of the small areas of attachment of neighboring particles and a minor amount of grain coarsening (i.e. an increase in size from ∼1 μm in the raw powder to ∼5 μm). In contrast, pores are not observed in $Ba(Zn_{1/3}Ta_{2/3})O_3$ samples prepared using conventional powder processing techniques when sintered under the same conditions (Fig. 3(b)). Furthermore, the sample prepared using conventional powder processing techniques sintered at lower temperatures (1520 °C) exhibits significant grain growth (i.e. a grain size twice than that (∼16 μm) of the ceramic injection moulded sample processed under the same conditions).

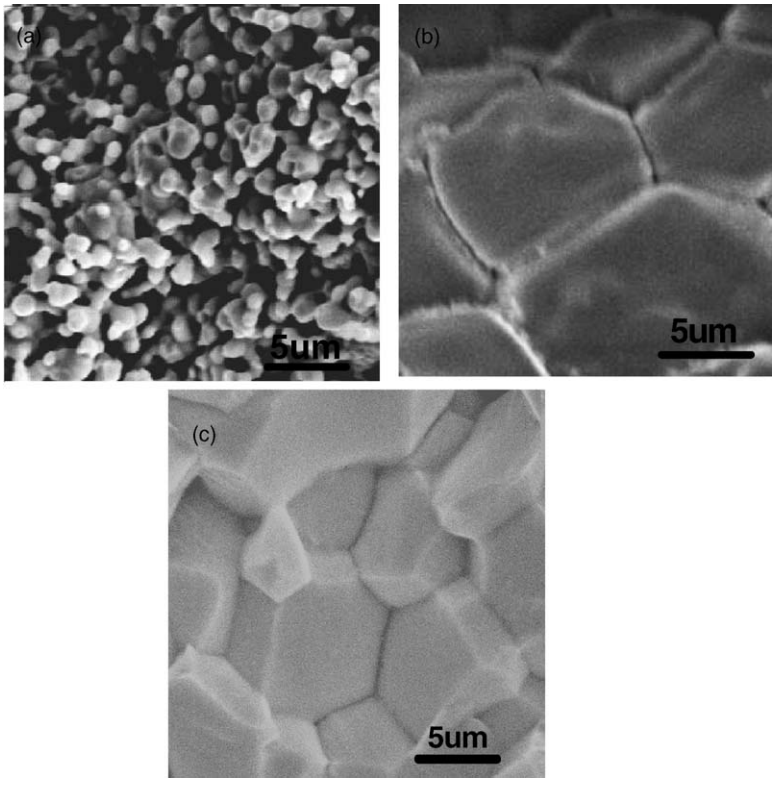

Fig. 3. SEM photomicrograph of: (a) ceramic injection moulded Zr- and Ni-doped $Ba(Zn_{1/3}Ta_{2/3})O_3$ sintered at 1520 °C; (b) Zr- and Ni-doped $Ba(Zn_{1/3}Ta_{2/3})O_3$ prepared using conventional powder processing methods sintered at 1520 °C; and (c) ceramic injection moulded Zr- and Ni-doped $Ba(Zn_{1/3}Ta_{2/3})O_3$ sintered at 1680 °C.

Thus, the significant grain growth is an important factor in the densification of pressed sample.[16]

Fig. 3(c) shows an SEM micrograph of a ceramic injection moulded sample with an average grain size of ~8 μm that was prepared by sintering at 1680 °C. Similar to the pressed samples, no obvious large pores are visible, as might be expected given its high density. Thus, to achieve enough high density ceramic injection moulded samples; a very high sintering temperature is required. Factors that affect the kinetics of processing such as the sintering time and atmosphere must be carefully controlled to minimize the loss of volatile Zn and its compounds. It might also be possible to choose additives that facilitate densification and reduce the required sintering temperature as a result of the liquid sintering mechanism, as we have accomplished for $Ba(Cd_{1/3}Ta_{2/3})O_3$, a similar perovskite compound.[17]

3.2. Dielectric properties of ceramic injection moulded $Ba(Zn_{1/3}Ta_{2/3})O_3$

Fig. 4 shows $Q \times f$ (quality factor times frequency) of ceramic injection moulded $Ba(Zn_{1/3}Ta_{2/3})O_3$ ceramics as a function of sintering temperatures. It is noteworthy that relatively high quality factors are achieved even in the absence of any direct evidence for Zn/Ta B-site ordering in the XRD patterns. The realization of high Qs in the absence of ordering is similar to that found for Zr-doped $Ba(Zn_{1/3}Ta_{2/3})O_3$ samples prepared by conventional powder processing methods.[4] As noticed, the relationship between $Q \times f$ values and sintered temperatures reveals the same trend as that between density and temperature. The highest $Q \times f$ value corresponds to the highest sintering density.

The $Q \times f$ values of the sintered $Ba(Zn_{1/3}Ta_{2/3})O_3$ ceramics ranged from ~16,000 to ~63,350. In contrast, the Zr- and Ni-doped $Ba(Zn_{1/3}Ta_{2/3})O_3$ ceramics prepared by conventional powder processing methods that were sintered at 1520 °C for 48 h shows higher $Q \times f$ products(~95,000). Further investigation is necessary to clarify the difference in the microwave performance between ceramic injection moulded and pressed $Ba(Zn_{1/3}Ta_{2/3})O_3$ samples.

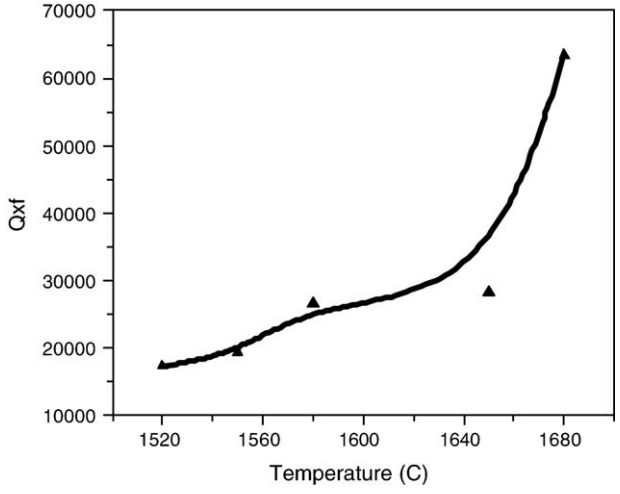

Fig. 4. Dependence of the $Q \times f$ product on the sintering temperature for ceramic injection moulded Zr- and Ni-doped $Ba(Zn_{1/3}Ta_{2/3})O_3$.

There is no obvious difference in the dielectric constant (~30) of Ni- and Zr-doped $Ba(Zn_{1/3}Ta_{2/3})O_3$ samples prepared with conventional processing methods sintered at 1520 °C and ceramic injection moulded samples sintered at 1650 °C for the same 48 h. The dependence of the temperature coefficient of resonant frequency on the sintering temperature for ceramic injection moulded Zr- and Ni-doped $Ba(Zn_{1/3}Ta_{2/3})O_3$ samples is shown in Fig. 5. A near zero temperature coefficient of resonant frequency was achieved for samples sintered at 1680 °C for 48 h. A maximum temperature coefficient of resonant frequency value of ~1.4 ppm/°C is observed after sintering at 1580 °C. In contrast, a near-zero (0.1 ppm/°C) temperature coefficient of resonant frequency for a $Ba(Zn_{1/3}Ta_{2/3})O_3$ sample with the same composition prepared using conventional powder processing could be achieved. The dependence of τ_f on sintering temperature did not show the same trends as that of $Q \times f$ and density. Earlier experimental results have also found that τ_f can depend on synthesis parameters.[18,19] For example in ABO_3 perovskites, τ_f can be directly correlated to the nature and extent of B-site ordering, as reported in a study of $Ba_xSr_{1-x}(Zn_{1/3}Nb_{2/3})O_3$.[20] As the order–disorder transition in $Ba(Zn_{1/3}Ta_{2/3})O_3$ (1500–1625 °C)[21] falls in the range of the sintering temperatures used in our study, the changes in τ_f with sintering temperature may be attributed to variation in the type and extent of ordering. Note that large changes in the degree of ordering as monitored by X-ray diffraction in our study were not found. This technique is, however, known to have limited sensitivity for detecting this effect, especially since the extent of ordering and the total volume of the ordered phases may be small. Earlier work by Davies et al. had reported ordering in regions at and near the grain boundary in $Ba(Zn_{1/3}Ta_{2/3})O_3$ which would be difficult to detect with X-ray diffraction.[22] The presence of secondary phases can also significantly influence τ_f. We did not find evidence for secondary phases in XRD resulting from the evaporation of zinc during the elevated sintered temperature (1680 °C) used in this study. However, we do need to

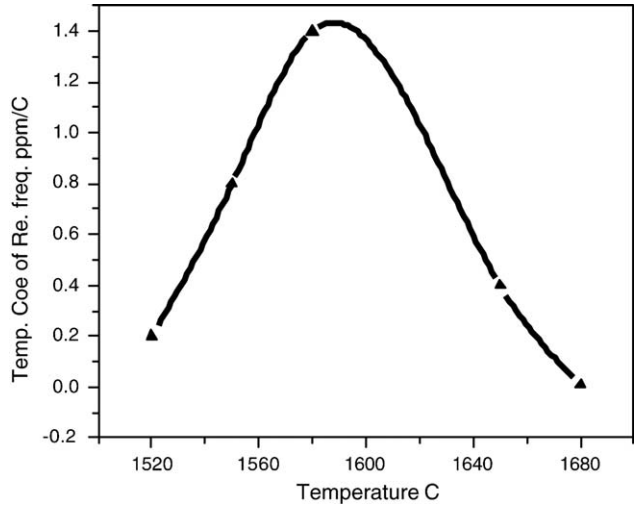

Fig. 5. Dependence of the temperature coefficient of resonant frequency on the sintering temperature for ceramic injection moulded Zr- and Ni-doped $Ba(Zn_{1/3}Ta_{2/3})O_3$.

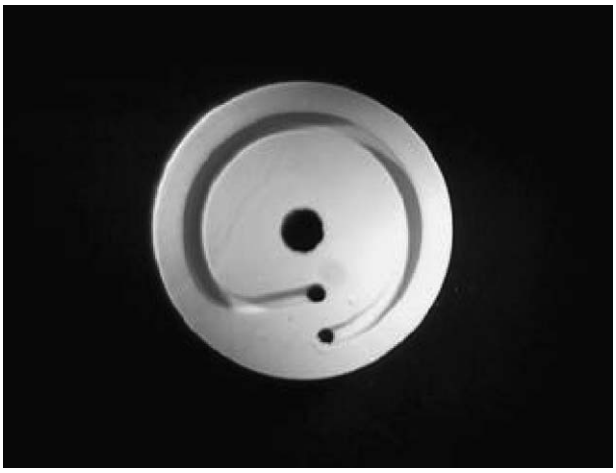

Fig. 6. Black and white photograph of a Möbius resonator synthesized from Zr- and Ni-doped $Ba(Zn_{1/3}Ta_{2/3})O_3$ using ceramic injection moulding. The sample itself has a light yellow color.

note that the secondary phases that constitute a small volume fraction, are randomly oriented and/or are possibly defective in nature can also be very difficult to detect.

Although the physical mechanism(s) responsible for changes in τ_f are just being uncovered, a number of workers have shown that variations can be correlated with structural parameters.[20,23,24] For example, Colla et al.[20] reported an empirical correlation between τ_f and the extent of octahedral tilting in perovskites. It is clear that to uncover the fundamental issues related to τ_f, further investigation is needed.

3.3. Dielectric-loaded Möbius bandpass filter

Fig. 6 shows a dual-mode Möbius resonators fabricated from Ni- and Zr-doped $Ba(Zn_{1/3}Ta_{2/3})O_3$ prepared by ceramic injection moulding. Fig. 7 shows a schematic drawing of the Möbius wire resonator structure. The structures consisted of two parallel Au loops recessed into grooves in the $Ba(Zn_{1/3}Ta_{2/3})O_3$. With

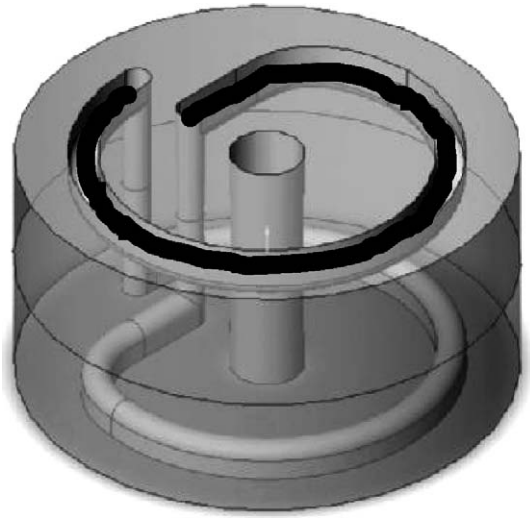

Fig. 7. Schematic drawing of the dielectric-loaded Möbius wire resonator illustrating the geometry of the dual mode Möbius resonator.

Table 1
Resonant frequency and Q of the dielectric-loaded Möbius wire resonator

Sample	Resonant frequency (GHz)	Q
1#	1.2507	928
2#	1.2888	954

Note that the Q is smaller than anticipated from the dielectric alone as a result of losses in the gold wire.

the $Ba(Zn_{1/3}Ta_{2/3})O_3$-loaded Möbius wire resonator inserted into the copper cavity, the weakly coupled microwave response was measured. Two matched $Ba(Zn_{1/3}Ta_{2/3})O_3$-loaded Möbius wire resonators were fabricated during the same sintering run. Table 1 shows that they have very similar microwave properties. A small difference in center frequency is found and probably arises from differences in the air gaps between the wire and the groove due to the imperfect fit. This is not surprising since the recessed gold wires were inserted into the grooves manually.

4. Conclusion

In this report, we described the synthesis methods and the structural, chemical and dielectric properties of $Ba(Zn_{1/3}Ta_{2/3})O_3$ ceramics produced using ceramic injection moulding. A high sintering density (~94%) was achieved using a high temperature (1680 °C) and extended (48 h) sintering process. The best samples to date exhibit a dielectric constant, ε_r, of ~30, a Q value of ~31,250 at 2 GHz, and a temperature coefficient of resonance frequency, τ_f, of 0.1 ppm/°C.

Acknowledgment

The Office of Naval Research under Contract N000140010550, N00014040461, the Office of Army Research under Contract W911NF0410376, the semiconductor research corporation (SRC) under research ID 2004-KJ-1201 and the ASU Wintech center supported this work. We would also like to thank David Cruickshank and Mike Hill of Trans-tech for interesting discussions on this mechanism responsible for changes of the temperature coefficient of resonant frequency.

References

1. Wakino, K., Nishikawa, T., Ishikawa, Y. and Tamura, H., Dielectric resonator materials and their application for mobile communication systems. *Br. Ceram. Trans. J.*, 1990, **89**, 39.
2. Rong, G., Newman, N., Shaw, B. and Cronin, D., Role of Ni and Zr doping on the electrical, optical, magnetic, and structural properties of barium zinc tantalate ceramics. *J. Mater. Res.*, 1999, **14**, 4011–4020.
3. Negas, T., Yeager, G., Bell, S. and Amren, R., Chemistry of electronic ceramic materials. In *Proceedings of the International Conference*, 1990, p. 21.
4. Tamura, H., Konoike, T., Sakabe, Y. and Wakino, K., Improved high-Q dielectric resonator with complex perovkite structure. *J. Am. Ceram. Soc.*, 1984, **67**, 59–61.
5. Chartier, T., Delhomme, E., Baumard, J. F., Veltl, G. and Ducloux, F., Injection moulding of hollow silicon nitride parts using fusible alloy cores. *Ceram. Int.*, 2001, **27**, 821–827.

6. Lin, S. I.-En., Near-net-shape forming of zirconia optical sleeves by ceramics injection moulding. *Ceram. Int.*, 2001, **27**, 205–214.
7. With, G. and Withbreuk de., N. M., Injection moulding of zirconia (Y-TZP) ceramics. *J. Eur. Ceram. Soc.*, 1993, **12**, 345–351.
8. Krug, S. J., Evans, R. G. and ter Maat, J. H. H., Residual stresses and cracking in large ceramic injection mouldings subjected to different solidification schedules. *J. Eur. Ceram. Soc.*, 2000, **20**, 2535–2541.
9. Shaw, H. M. and Edirisinghe, M. J., Shrinkage and particle packing during removal of organic vehicle from ceramic injection mouldings. *J. Eur. Ceram. Soc.*, 1995, **15**, 109–116.
10. Pond, J. M., Liu, S. and Newman, N., Dual-mode and quad-mode Möbius resonators. *IEEE MTT-S Int. Microwave Symp. Dig.*, 2000, **3**, 1771–1774.
11. Pond, J. M., Liu, S. and Newman, N., Band pass filters using dual-mode and quad-mode Möbius resonators. *IEEE Trans. MTT*, 2001, **49**, 2363–2368.
12. Liu, D. M. and Tseng, W. J., Influence of debinding rate, solid loading and binder formulation on the green microstructure and sintering behaviour of ceramic injection mouldings. *Ceram. Int.*, 1998, **24**, 471–481.
13. Li, Y., Liu, S., Qu, X. and Huang, B., Thermal debinding processing of 316L stainless steel powder injection molding compacts. *J. Mater. Proc. Tech.*, 2003, **6487**, 1–5.
14. Huang, C. L., Chiang, K. H. and Chuang, S. C., Influence of V_2O_5 additions to $Ba(Mg_{1/3}Ta_{2/3})O_3$ ceramics on sintering behavior and microwave dielectric properties. *Mater. Res. Bull.*, 2004, **39**, 629–636.
15. Rhodes, W. H., Agglomerate and particle size effects on sintering yttria-stabilized zirconia. *J. Am. Ceram. Soc.*, 1981, **64**, 19–22.
16. Chang, Y. M., Birnie, D. P. and Kingery, W. D., *Physical Ceramics: Principles for Ceramic Science and Engineering*. John Wiley & Sons, New York, 1997, pp. 371–388.
17. Liu, S., Sun, J., Taylor, R., Smith, D. J. and Newman, N., Microstructure and dielectric properties of $Ba(Cd_{1/3}Ta_{2/3})O_3$ microwave ceramics synthesized with a boron oxide sintering aid. *J. Mater. Res.*, 2004, **19**, 3526–3533.
18. Chen, H. C., Weng, M. H., Horng, J. H., Houng, M. P. and Wang, Y. H., Effect of bismuth addition on sintering behavior and microwave dielectric properties of zinc titanate ceramics. *J. Electron. Mater.*, 2005, **34**, 119.
19. Chu, S. Y. and Chen, T. Y., Fabrication of modified lead titanate piezoceramics with zero temperature coefficient and its application on SAW devices. *IEEE Trans. Ultrason. Ferroelectr. Freq. Control.*, 2004, **51**, 663–667.
20. Colla, E. L., Reaney, I. M. and Setter, N., Effect of structural changes in complex perovskites on the temperature coefficient of the relative permittivity. *J. Appl. Phys.*, 1993, **74**, 3414–3425.
21. Reaney, I. M., Qazi, I. and Lee, W. E., Order-disorder behavior in $Ba(Zn_{1/3}Ta_{2/3})O_3$. *J. Appl. Phys.*, 2000, **88**, 6708–6714.
22. Davies, K. P., Tong, J. and Negas, T., Effect of ordring-induced domain boundaries on low-loss $Ba(Zn_{1/3}Ta_{2/3})O_3$–$BaZrO_3$ perovskite microwave dielectrics. *J. Am. Ceram. Soc.*, 1997, **80**, 1727–1740.
23. Reaney, I. M., Colla, E. L. and Setter, N., Dielectric and structural characteristics of Ba- and Sr-based complex perovskites as a function of tolerance factor. *Jpn. J. Appl. Phys.*, 1994, **33**, 3984–3990.
24. Reaney, I. M., Wise, P. and Ubic, R. R., On the temperature coefficient of resonant frequency in microwave dielectrics. *Philos. Mag. A*, 2001, **81**, 501–510.